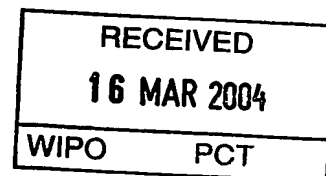


BUNDESREPUBLIK DEUTSCHLAND

**PRIORITY
DOCUMENT**

SUBMITTED OR TRANSMITTED IN
COMPLIANCE WITH RULE 17.1(a) OR (b)



Prioritätsbescheinigung über die Einreichung einer Patentanmeldung

EP/03/14679
102 59 874.6

Aktenzeichen:

102 59 874.6

Anmeldetag:

20. Dezember 2002

Anmelder/Inhaber:

Julius-Maximilians-Universität Würzburg,
97070 Würzburg/DE

Bezeichnung:

Optische Messung der Aktivierung von
G-Protein gekoppelten Rezeptoren

IPC:

noch nicht festgelegt

Die angehefteten Stücke sind eine richtige und genaue Wiedergabe der ursprünglichen Unterlagen dieser Patentanmeldung.

München, den 10. Februar 2004
Deutsches Patent- und Markenamt
Der Präsident
Im Auftrag

Dzierzon

BEST AVAILABLE COPY

Zusammenfassung

G-Protein-gekoppelte-Rezeptoren vermitteln über nachgeschaltete Signalwege zelluläre Antworten auf eine Vielzahl von extrazellulären Botenstoffen wie Hormone oder Neurotransmitter. Diese Rezeptorfamilie ist die wichtigste Zielgruppe von existierenden und zu entwickelnden Arzneimitteln. Wir beschreiben hier die Entwicklung und Erprobung einer Methode, die Liganden-induzierte Aktivierung dieser Rezeptoren direkt am Rezeptormolekül selbst zu detektieren. Das vorgestellte Verfahren beruht auf der Detektion von Liganden-induzierter Konformationsänderungen mit Hilfe intramolekularer Distanzmessungen. Die Messung der Rezeptoraktivierung kann ubiquitär für alle G-Protein gekoppelten Rezeptoren einschließlich Orphan-Rezeptoren eingesetzt werden und ermöglicht zeitlich hochaufgelöste Messungen auch in intakten Zellen. Da Konformationsänderungen in den Rezeptoren selbst gemessen werden, kann die Wirkung von Agonisten, partiellen Agonisten und Antagonisten unterschieden werden.

Direkte Messung der Aktivierung von G-Protein gekoppelten Rezeptoren

Die Erfindung bezieht sich auf die optische Messung der Aktivierung von

5 Membranrezeptoren aus der Familie der G-Protein gekoppelten Rezeptoren (GPCR).

Diese Rezeptoren vermitteln über nachgeschaltete Signalwege adäquate zelluläre

Antworten auf extrazelluläre Stimuli wie Licht, Odorantien, Hormone oder

Neurotransmitter. Aufgrund der Existenz einer Vielzahl von Rezeptoren und ihrer

prominenten Stellung bei der Regulation zellulärer Signale sind GPCR die wichtigste

Zielgruppe von Arzneistoffen. Folgende Methoden sind verfügbar um die Interaktion potentieller Liganden mit dem Rezeptor zu studieren:

a. Liganden-Bindungsassays. Bei dieser Methode ist man auf verfügbare Radioaktiv-
oder Fluoreszenz-markierte Liganden angewiesen. Dies limitiert die Anwendung auf
15 bekannte Rezeptoren. Die Wirkung des zu untersuchenden Liganden auf den GPCR
(Aktivierung oder Inhibierung) kann nicht bestimmt werden.

b. Die Messung der Aktivität von den GPCR nachgeschalteten Effektorsystemen ist
bisher die wichtigste Methode für das „drug screening“. Aufgrund dieses indirekten
Meßprinzips treten gravierende Nachteile auf:

20

1. Der Existenz unspezifischer Arzneimitteleffekte, die nicht über den zu untersuchenden
GPCR vermittelt wurden, wie z.B. Effekte an den Signalmolekülen die dem Rezeptor
nachgeschaltet sind oder Effekte über andere GPCR, die diesen Signalweg parallel
regulieren können.

25

2. Die Rezeptoraktivierung und Deaktivierung kann nicht in Echtzeit bestimmt werden und damit sind Rezeptoraktivierung und Rezeptordesensibilisierung nicht klar zu trennen.

5 3. Die Messung der GPCR Aktivität hängt von der Expression und Spezifität der nachgeschalteten G-Proteine und Effektoren ab, die potentiell von den zu untersuchenden Arzneistoffen moduliert werden könnte. Dies verhindert exakte Vergleichstudien zwischen Rezeptorsubtypen.

4. Die Stärke des Signals hängt von der Anzahl der exprimierten Rezeptoren ab. Unkontrollierbare Schwankungen in der Expression beeinflussen das Meßergebnis.

5. Es fehlt die Möglichkeit Agonismus, partiellen Agonismus, inversen Agonismus und neutralen Antagonismus direkt am Rezeptormolekül zu messen.

15 6. Nach der Entdeckung, daß eine Vielzahl von GPCR dimerisieren oder oligomerisieren können wurde erstmals versucht direkt die Aktivierung der Rezeptoren durch intermolekulare Änderungen von Bioillumineszenz- oder Fluoreszenz- Resonanz-Energie-Transfer (BRET oder FRET) zu messen. Allerdings war bei der
20 überwältigenden Mehrheit keine Beeinflußung der Meßgröße durch Liganden feststellbar.

7. Ein weiterer Ansatz die GPCR direkt zu messen beruht auf Fluoreszenz-Quenching Effekte die durch Konformationsänderungen des Rezeptors moduliert werden. Diese
25 Methode erlaubte erstmals Liganden-induzierte Konformationsänderungen eines aufgereinigten und chemisch Fluorescein-markierten GPCR zeitlich zu messen, ergab

allerdings Aktivierungszeitkonstanten, die mehr als hundertfach langsamer waren als dies aufgrund physiologischer Daten zu erwarten gewesen wäre.

Die zu patentierende Idee, die unserer Erfindung zugrunde liegt, ist die - der Liganden-induzierten Aktivierung zugrundeliegende - intramolekulare Konformationsänderung des GPCR mit Hilfe von optischer Distanzmessung meßbar zu machen. Als optisches Meßprinzip einsetzbar ist beispielsweise die Detektion von BRET oder FRET dessen erfolgreiche Anwendung im beiliegenden Manuskript demonstriert wurde. Im Unterschied zu den unter c. und d. beschriebenen Verfahren beruht unsere Methode auf der Verwendung von mehr als einem intramolekularen Referenzpunkt für die optische Distanzmessung. Beispielsweise konnten wir zwei Domänen auf GPCR ermitteln, die während der Rezeptoraktivierung ihre Distanz zueinander ändern (siehe Manuskript). In diesen beiden Domänen wurden dann jeweils ein Chromophor inseriert und die Distanzänderung zwischen den Chromophoren während der Aktivierung der Rezeptoren wurde mit Hilfe von Änderungen des FRET meßbar gemacht. Um diese Methode für lebende Zellen nutzbar zu machen wurden FRET-taugliche genetisch codierte Farbstoffe wie das cyan-fluorescent- und das yellow-fluorescent- protein (CFP, YFP) an den aktivierungssensitiven Domänen von GPCR inseriert (Ref). Nach Optimierung dieser FRET-basierten Methode zur direkten Bestimmung von Rezeptoraktivität am Beispiel des Parathormon-Rezeptors wurde dieses Meßprinzip an weiteren Rezeptoren wie z.B. den α_{2A} -Adrenergen Rezeptor erfolgreich verifiziert.

Die Methode, mit Hilfe durch optische Distanzmessung detektierte intramolekulare Konformationsänderungen des GPCR die Liganden-induzierte Regulation von GPCRs direkt zu messen soll insbesondere für die Anwendung beim Screening und bei der Charakterisierung von neu zu entwickelnden und existierenden Pharmaka patentiert

werden. Diese Methode eignet sich aufgrund des Meßprinzips für die Anwendung allen existierenden GPCR und soll auch dafür patentiert werden. Folgende Vorteilen gegenüber den bislang verfügbaren Methoden mögen bei der Patentierung berücksichtigt werden:

1. Entwicklung von Arzneimitteln die über Orphan GPCR wirken: Bei der Messung der Rezeptoraktivität auf Ebene des Rezeptors ist es unwichtig an welches G-Protein und Effektorsystem der Rezeptor koppelt.
2. Weniger unspezifische Pharmakaeffekte (false-positives): Durch die Meßung der Liganden-(Arzneimittel-) induzierten Konformationsänderung des GPCRs werden unspezifische Arzneimittelleffekte, die nicht über den zu untersuchenden GPCR vermittelt wurden, wie z.B. Effekte an den Signalmolekülen die dem Rezeptor nachgeschaltet sind oder Effekte über andere GPCR, die diesen Signalweg parallel regulieren können von vornherein ausgeschaltet.
3. Die Rezeptoraktivierung und Deaktivierung kann in Echtzeit bestimmt werden. Dadurch kann die Kinetik der Liganden-Rezeptor-Interaktion und somit auch die Affinität des Liganden zu Rezeptor direkt bestimmt werden. Weiterhin sind Rezeptoraktivierung und nachfolgende Regulationsprozesse wie z.B. Rezeptordesensibilisierung klar zu trennen (Ref).
4. Die Messung der GPCR Aktivität hängt nicht von der Expression und Spezifität der nachgeschalteten G-Proteine und Effektoren ab, die potentiell von den zu untersuchenden Arzneistoffen moduliert werden könnte. Dadurch werden exakte Vergleichstudien zwischen verschiedenen Liganden oder Rezeptorsubtypen ermöglicht.

5. Die Stärke des Signals der Rezeptoraktivierung hängt nicht von der Anzahl der exprimierten Rezeptoren ab. Dadurch wird das Meßergebnis frei von Ungenauigkeiten, die auf unkontrollierbare Schwankungen in der Expression zurückzuführen sind.

5

6. Die Möglichkeit Agonismus, partiellen Agonismus, inversen Agonismus und neutralem Antagonismus direkt am Rezeptormolekül zu messen wird eröffnet.

A millisecond activation switch for G protein-coupled receptors in living cells

Jean-Pierre Vilardaga*, Moritz Bünemann*, Cornelius Krasel, Mariàn Castro and
Martin J. Lohse

*Institute of Pharmacology and Toxicology, University of Würzburg, Versbacher Str. 9,
D-97078 Würzburg, Germany*

**These authors contributed equally to this work*

tel. ++49-931-201 48400 fax ++49-931-201 48539

email: lohse@toxi.uni-wuerzburg.de

Running title: Watching dynamics in G protein coupled receptors

(34877 characters)

Abstract

Hormones and neurotransmitters transduce signals via G-protein-coupled receptors as key switches in order to change cellular functions. Despite utilizing common signalling pathways, hormone and neurotransmitter responses exhibit different temporal pattern. To reveal the molecular basis for such differences we developed a generally applicable fluorescence-based technique for real-time monitoring of the activation switch for G protein-coupled receptors in single cells. We used such direct measurements to investigate the activation of the α_{2A} -adrenergic (neurotransmitter) and the parathyroid hormone (PTH, hormone) receptors and observed kinetics that were much faster than previously thought: ≈ 40 ms for the α_{2A} -adrenergic receptor and ≈ 1 s for the PTH receptor. The different switch times are in agreement with the distinct biological functions of these receptors. Agonist, partial agonist and antagonist could rapidly switch on and off the receptor in proportion to their respective intrinsic activities. These measurements permit the comparison of agonist and partial agonist intrinsic activities at the receptor itself and provide evidence for millisecond activation times of G-protein coupled receptors.

Introduction

G-protein-coupled receptors (GPCRs) are the largest family of hormone or neurotransmitter receptors; they have a common structure containing seven transmembrane α -helices (Rohrer *et al.*, 1998; Gether *et al.*, 2000; Pierce *et al.*, 2002). Their activation by specific agonists – hormones or neurotransmitters – switches them into an active state that couples to and activates G-proteins, the signal transducers. The G-proteins, in turn, can activate a multitude of effector proteins such as ion channels or 2nd messenger producing enzymes that alter many functions (e.g., cardiovascular, neural, endocrine) in virtually every type of cells. A large body of data suggests that agonist-induced activation leads to a relative rearrangement of the receptor's transmembrane helices, most notably of helix III and VI (Farrens *et al.*, 1996; Sheikh *et al.*, 1996 and 1999; Wieland *et al.*, 1996; Ward *et al.*, 2002).

A very special GPCR is the "light receptor" rhodopsin that senses light by using a covalently coupled ligand, 11-cis retinal, that isomerizes upon capture of a photon. In this case, conformational changes in the "receptor" protein can be inferred from spectroscopic studies of the bound retinal, and multiple activation states formed within milliseconds have been described (Farrens *et al.*, 1996; Okada *et al.*, 2001). No comparable techniques are available for hormone- or transmitter-activated receptors. Spectroscopic studies have been done with purified β_2 -adrenergic receptor chemically labelled with fluorophores and reconstituted into lipid membranes (Gether *et al.*, 1995; Jensen *et al.*, 2001; Ghanouni *et al.*, 2001a and 2001b). These studies observed agonist-mediated fluorescence changes in the minute time scale. This is much slower than biological responses to receptor activation, which can occur within seconds. Here, we set out to devise a new fluorescence approach to observe with a high resolution the conformational switch of receptor activation in living cells.

We used two models of GPCRs – the parathyroid hormone receptor (PTHr), which is a member of the class 2 GPCRs (Bockaert and Pin, 1999) and binds the large hormone PTH (MW \approx 3700), and the α_{2A} -adrenergic receptor, which is a class 1 GPCR (Bockaert and Pin, 1999) and binds noradrenaline, a small (MW= 169) neurotransmitter. The PTHr transmits its signals to the G-proteins G_s and G_q , and thereby causes increases in the 2nd messengers cAMP and inositol trisphosphate; the α_{2A} -adrenergic receptor couples to G_i and G_o and thereby decreases cAMP and regulates N-type Ca^{2+} - and GIRK channels. Since activation of receptors including the PTHr is thought to involve a change in the relative positions of the cytoplasmic parts of transmembrane helices III and VI (Sheikh *et al.*, 1999; Vilardaga *et al.*, 2001), we reasoned that a movement of helix VI should be transmitted to the third intracellular loop of the receptor.

To monitor such movements we generated a series of receptor mutants into which the cyan- and yellow-emitting variants of the green fluorescent protein (i. e., CFP and YFP reviewed in Tsien, 1998; Miyawaki and Tsien, 2000) were inserted at various positions of the third intracellular loop and/or of the carboxy-terminus of the two receptors, respectively. We report here the generation of such mutants and their use to monitor receptor activation.

Results and discussion

Generation of receptor constructs with agonist-sensitive FRET

A series of receptor constructs were generated that carried CFP and/or YFP in various positions of the third intracellular loop and/or of the carboxy-terminus of the PTHR and the α_{2A} AR, respectively. The two constructs showing the best cell surface expression, pharmacological properties and agonist sensitivity were further used in this study and are referred to as receptor cameleons PTHR-cam and α_{2A} AR-cam (Figure 1A).

Emission fluorescence spectra were recorded from HEK293 cells stably expressing PTHR-cam and various control constructs. Excitation of a PTHR carrying only a CFP-moiety in its 3rd intracellular loop (PTHR-CFP_{3-loop}) with light at 436 nm resulted in an emission at 480 nm (corresponding to the CFP emission, Figure 1B). The additional presence of YFP in the carboxy terminus (PTHR-cam) lead to a reduced emission at 480 nm plus a strong emission at the characteristic wavelength of YFP (535 nm, Figure 1B). Photobleaching of the acceptor confirmed that the latter emission was due to FRET (see Figure 1C). The presence of YFP in the C-terminus alone (PTHR-YFP_{C-term}) did not result in significant emission at 535 nm when excited at 436 nm (Figure 1B). Receptor constructs containing only YFP showed no specific emission peak at 535 nm when excited at 436 nm (Figure 1B).

Signals recorded from single HEK293 cells expressing PTHR-cam were then analysed at emissions of 480 nm (CFP) and 535 nm (YFP) upon excitation at 436 nm (CFP excitation). The microscopic illumination allowed photobleaching experiments in order to verify that the emission at 535 nm was indeed due to FRET. After bleaching of the acceptor in the PTHR-cam construct with intense light at 480 nm, the emission at 480 nm increased by 50±3% together with a more than 5-fold reduction of the 535 nm

emission (Figure 1C). Similar spectral and photobleaching data were obtained with the α_2A AR-cam stably expressed in HEK293 cells (data not shown).

We then investigated the effects of the agonist PTH on the FRET signal of PTHR-cam, measured as the background-corrected emission intensity ratio F_{535}^*/F_{480}^* . After addition of 1 μ M PTH, the ratio F_{535}^*/F_{480}^* rapidly decreased (Figure 1D). After a short delay (≈ 600 ms) the decrease followed a mono-exponential time-course with a time-constant $\tau = 3.00 \pm 0.25$ s ($n=9$). The symmetrical increase in CFP emission and decrease in YFP emission indicate that the change was due to a decrease in FRET. Control experiments with co-expression of PTHR-CFP_{3-loop} and PTHR-YFP_{C-term} showed no FRET in the absence or in the presence of PTH (1 μ M) and thus made it unlikely that the signals resulted from *intermolecular* FRET in receptor dimers (data not shown). It should be noted, however, that the *intramolecular* nature of this signal does not exclude the presence of receptor dimers.

Similarly, α_2A AR-cam showed intramolecular FRET, and again the specific agonist, i.e. noradrenaline, caused a decline of the FRET signal (see Figures 3, 4, 6). Virtually identical results were obtained with the two receptors expressed in other cell lines (CHO, PC12; data not shown). The agonist-induced decreases in FRET in the two types of receptors suggest that the agonist-induced conformational switch is similar in class 1 and class 2 GPCRs. Because of the location of the CFP and YFP in the receptors (Figure 1A) they are compatible with a movement of the 3rd intracellular loop away from the C-terminus as predicted by computer simulations of the α_{1B} -adrenergic receptor (Greasley *et al.*, 2001).

Pharmacological characterization of the receptor-cameleon

The receptor-cameleon constructs stably expressed in HEK293 cells retained the typical ligand binding which was of somewhat lower affinity than for the corresponding wild-type receptors (Figure 2): the PTH affinity was $K_i=15.5\pm0.9$ nM for PTHR-cam and $K_i=2.4\pm0.4$ nM for PTHR; the norepinephrine affinity was $K_i=5.0\pm0.8$ for $\alpha_{2A}AR$ and $K_i=16.7\pm1.4$ μ M for $\alpha_{2A}AR$ -cam. PTHR-cam and $\alpha_{2A}AR$ -cam signalled efficiently to adenylyl cyclase ($EC_{50}=12.8\pm1.4$ nM) and to the GIRK channel ($EC_{50}=1.08\pm0.01$ μ M), respectively (Figure 2A-B). Note that the difference in the signal amplification between wild type- and cam receptors is in part due to the higher expression level of the wild type receptors (1.01×10^6 vs 0.34×10^6 receptors/cells for PTHR and PTHR-cam, respectively; 24 and 6 pmol/mg for $\alpha_{2A}AR$ and $\alpha_{2A}AR$ -cam, respectively). Finally, confocal microscopy showed that the majority of PTHR-cam and $\alpha_{2A}AR$ -cam receptors in stably transfected cells were correctly present at the cell surface (Figure 2C). These data indicate that both receptor constructs were properly targeted to the cell surface upon expression in HEK293 cells and retained essential binding properties as well as significant G-protein-mediated signalling of the corresponding wild-type receptors. Similar data were obtained upon expression in various cell lines (e.g. CHO; data not shown)

The agonist-mediated FRET signal is coupled to receptor activation

How can we be sure that the agonist-induced changes in FRET do indeed reflect the conformational change of the receptor? We sought to answer this critical question along several lines.

First, we set out to prove that the FRET signal was indeed caused by the receptors themselves and not by interactions with other proteins such as G-proteins or β -arrestins. Therefore, we studied PTHR-cam under conditions that exclude interactions with these proteins. In isolated cell membranes prepared from HEK293 cells stably expressing PTHR-cam – i.e. in the absence of cytosolic proteins – the PTH-induced signal had the same magnitude as in intact cells (Figure 3A). Further stripping the cell membranes with 6 M urea – a treatment known to leave GPCRs intact but to denature virtually all other proteins (Sheikh *et al.*, 1999; Lim and Neubig 2001) – did also not affect the magnitude of the PTH-induced signal at saturating concentrations (Figure 3A). And finally, inactivating G_i and G_o with pertussis toxin in cells expressing the α_{2A} AR-cam did not affect the noradrenaline-induced FRET signal (data not shown), indicating that the signal was not due to a receptor/G-protein interaction. Taken together, these data strongly indicate that the FRET signals were not caused by interactions of the receptors with other proteins.

Second, we wanted to prove that the FRET signals correspond to the activation state of the receptor. To do this, we investigated the effects of agonists and antagonists. A truncated variant of PTH, PTH7-34, which is a low affinity antagonist, failed to induce a change in FRET (Figure 3A). Similarly, noradrenaline (10 μ M) induced a rapid decrease of the FRET signal in the α_{2A} AR-cam (Figure 3B), while saturating concentrations of the high affinity α_2 -adrenergic receptor antagonist phentolamine (10 μ M) did not alter the FRET signal when given alone (not shown). However, phentolamine rapidly reverted the noradrenaline-induced signal (Figure 3B). This is compatible with its nature as a competitive antagonist. Thus, the rigorous agonist dependence on the change of the FRET signal mirrors the active state of the receptor.

Third, binding of G-proteins to receptors is known to enhance formation of the active, agonist-bound state. Because of the reduced ability of the receptor cameleons to

couple to G-proteins; such assays required the addition of exogenous G-proteins. After addition of purified G_o to membranes containing $\alpha_{2A}AR$ -cam, the agonist [3H]UK14304 bound with high affinity to the receptors ($K_d=3.4\pm0.8$ nM; Supplementary figure 1). Addition of the stable GTP-analog GTP γ S reduced this affinity ($K_d=9.6\pm1.1$ nM) indicative of a disruption of the high-affinity receptor/G-protein complex. GTP γ S reduced the binding of 5 nM [3H]UK14304 by more than 50% (Figure 3C *right* panel). Similarly, GTP γ S reduced the FRET signals caused by a 5 nM UK14304 in the same membrane preparation (i.e. in the presence of G_o) by more than 50% (Figure 3C *left* panel). GTP γ S did not affect the signal of saturating concentrations of UK14304 (data not shown), which is in agreement with the lack of effect of urea-treatment on the maximal PTH-induced signal obtained in membranes (Figure 3A). Taken together, these data suggest that the FRET-signal originates in the active conformation of the receptor itself, and that this active conformation binds to and is stabilized by G-proteins.

FRET changes mediated by a partial agonist

The FRET assay also properly reflected partial agonism (Figure 4): Compared to the full agonist noradrenaline, the high affinity partial agonist clonidine at saturating concentrations (10 μ M) gave a three-fold smaller FRET signal (Figure 4). Subsequent application of noradrenaline (10 μ M) still produced the full response. The simultaneous addition of clonidine (10 μ M) restored this response back to the partial response seen with clonidine alone; and again, after washout, noradrenaline still produced the full initial response. These data correspond exactly to the predicted properties of a high affinity partial agonist. However, compared to other assays used so far to detect partial agonism, the FRET assay is not dependent on transducer and effector proteins. Instead it reflects directly the partial agonist effects on the receptors themselves. Mechanistically, the ability of clonidine to partially reverse the agonist-mediated signal suggests that the

partial agonist restrains the complete movement between the 3rd intracellular loop and the C-terminus. This is compatible with the notion that the partial agonism process occurs at the receptor level by inducing a restrained conformational change within the agonist binding site (Ghanouni *et al.*, 2001).

Comparing receptor activation with desensitization

Receptor activation should precede receptor deactivation. Therefore, we measured the rate-limiting step in PTHR-deactivation (Villardaga *et al.*, 2002; Castro *et al.*, 2002), the association of β -arrestin with the receptor, again with a FRET-based approach. To this end, we co-expressed functional PTHR carrying CFP at its C-terminus (PTHR-CFP_{C-term}) and β -arrestin2 fused at its C-terminus to YFP (β -arrestin2-YFP). Measuring the appearance of FRET between the CFP and the YFP then monitored PTH-induced binding of β -arrestin2 to the receptor. The dynamics of this signal were compared with the receptor activation of PTHR-cam (Figure 5). The initial ratio F_{535}^*/F_{480}^* was 1.10 ± 0.05 for cells co-expressing PTHR-CFP_{C-term} and β -arrestin2-YFP. After addition of PTH (100 nM), the ratio increased by up to 32 ± 11 % with a $t_{1/2}$ of 150 ± 12.1 s ($n=8$), reflecting the PTH-mediated receptor/ β -arrestin2 association. The same concentration of PTH (100 nM) had a 5-fold faster effect on PTHR-cam, with a $t_{1/2}$ of 32 ± 1.9 s ($n=4$ experiments). Furthermore, the lag time between addition of PTH and the beginning of the response was about three times shorter for the activation signal (PTHR-cam) than for β -arrestin translocation (Figure 5, inset). Thus, the signal for receptor activation does indeed begin earlier and proceeds much faster than that for receptor deactivation.

Differential speed of activation between hormone and neurotransmitter receptors

Time-resolved determination of the FRET signals recorded from single cells after activation with various concentrations of PTH and noradrenaline, respectively, allowed the analysis of the switch kinetics (Figure 6). Under all conditions, the decrease of the ratio F_{535}^*/F_{480}^* followed a monoexponential time-course. Increasing concentrations of agonist resulted in shorter delay times as well as faster time-courses of the signals. At low agonist concentrations, the rate constants (k_{obs}) increased in proportion to agonist concentration (Figure 6B), indicating that agonist binding to the receptors was the rate-limiting step. At higher concentrations of agonist, the rate constants reached a maximum, suggesting that a step other than the collisional probability of agonist/receptor became rate-limiting. This step is most likely the agonist-mediated conformational switch of the receptors. The time constant required for the switching was less than 40 ms in the case of the $\alpha_{2A}\text{AR}$ -cam. This is more than 5000 times faster than the switch time measured for chemically labelled, purified β_2 -adrenergic receptors (Gether *et al.*, 1995; Jensen *et al.*, 2001; Ghanouni *et al.*, 2001a and 2001b) and corresponds well to the physiological requirements of neurotransmitter receptors. In contrast, the kinetics of the FRET-signal were 25-fold slower ($\tau \approx 1\text{s}$) for the PTH-receptor. This may be explained by the fact that PTH is a large agonist and that its binding appears to involve several contact points both in the extended N-terminus and in the core of the PTHR (Gardella and Jüppner, 2001).

The saturation of the k_{obs} -values together with the concentration-dependent delay times (Figure 6) are compatible with a simple two-step process of first-order agonist binding and subsequent receptor activation. The delay times indicate that the FRET signal is not induced by agonist binding but is due to the conformational switch. Mechanistically, this switch appeared to be similar in a class 1 and a class 2 GPCR, but it was much faster in the class 1 $\alpha_{2A}\text{AR}$ -cam. The slower switch time of the class 2 PTH receptor is compatible with the slow hormonal effects of PTH, compared with the fast synaptic action of noradrenaline. Millisecond switch times have so far been thought to

be limited to ion channel receptors (Chang and Weiss, 2002) or to rhodopsin (Okada *et al.*, 2001). However, our data indicate that also a neurotransmitter GPCR can be switched in the millisecond time scale, and they show that the extent of switching is dependent on the intrinsic efficacy of the ligand.

Materials and methods

Molecular biology and cell culture. Site-directed mutagenesis was performed on the human PTH/PTHrP receptor (PTHR) and the mouse α_{2A} -adrenergic receptor cDNAs. The cDNAs encoding the enhanced yellow- and cyan fluorescent protein (YFP and CFP) were fused to position G418 of the COOH-terminus of the PTHR and inserted between Gly395 and Arg396 into the third intracellular loop of the PTHR, respectively. For the α_{2A} -adrenergic receptor, YFP was inserted in the third intracellular loop between Ala250 and Ser371, and CFP was fused to Val461 in the C-terminus. Constructions were performed by polymerase chain reactions as described (Vilardaga *et al.*, 1995). β -Arrestin2-YFP was constructed following the procedure described for the construction of arrestin3-GFP (Groarke *et al.*, 1999). Constructions were verified by sequencing. Receptor cDNAs were cloned into pCDNA3 (Invitrogen) for transient and stable expression in mammalian cells. HEK293, CHO and PC12 cell lines served as the expression systems for the wild-type and chimeric receptors. The procedure for the selection of stable cell line has been previously described (Vilardaga *et al.*, 2001).

Pharmacology. Ligand binding, cAMP assays, measurement of α_{2A} -adrenergic receptor-activated GIRK currents and reconstitution of receptor- G_o coupling were measured as previously described (Vilardaga *et al.*, 2001 and 2002; Bünemann *et al.*, 2001; Richardson and Robishaw, 1999). Saturation and competition binding studies were analysed with the program Prism to calculate K_D - and K_i -values.

Electrophysiology. Whole cell GIRK currents were measured in HEK293 cells stably expressing 6 pmol/mg membrane protein α_{2A} -AR-cam 20-28h after transient transfection with GIRK1 and GIRK4 as described previously (Bünemann *et al.*, 2001). Membrane currents were recorded using an EPC 9 amplifier and Pulse software (HEKA

Instruments) for voltage control, data acquisition and data evaluation. Experimental conditions such as patch pipettes, internal and external solutions, voltage-clamp protocol as well as the superfusion system were the same as described previously (Bünemann *et al.*, 2001).

Fluorescence measurements. Cells were washed with PBS, scraped from the plate and resuspended in buffer A (137 mM NaCl, 5 mM KCl, 1 mM CaCl₂, 1 mM MgCl₂, 20 mM Hepes, 0.1% BSA, pH 7.4) at a density of $\approx 10^7$ cells/ml. Steady-state fluorescence emission spectra of the cells suspension were measured with a spectrofluorimeter (Perkin-Elmer) in cuvettes containing HEK293 cells expressing the indicated receptors, and were normalized to the respective maxima for PTHR-CFP_{3-loop} and PTHR-cam. PTHR-YFP_{C-term} was normalized relative to the maximal response upon exposure to 480 nm light.

FRET measurements. Cells grown on coverslips were maintained in buffer A at room temperature and placed on a Zeiss inverted microscope (Axiovert135) equipped with an oil immersion 63x objective and a dual emission photometric system (Till Photonics). Samples were excited with light from a polychrome IV (Till Photonics). In order to minimize photobleaching, the illumination time was set to 5 ms applied with a frequency between 1 and 75 Hz dependent on agonist concentration. FRET was monitored as the emission ratio of YFP to CFP, F_{535}/F_{480} , where F_{535} and F_{480} are the emission intensities at 535 ± 15 nm and 480 ± 20 nm (beam splitter DCLP 505nm) upon excitation at 436 ± 10 nm (beam splitter DCLP 460 nm). The emission ratio was corrected by the respective spill-over of CFP into the 535 nm channel (spill-over of YFP into the 480 nm channel was negligible) to give a corrected ratio F_{535}^*/F_{480}^* . FRET between CFP and YFP in cells stably expressing the receptor constructs was also determined by donor recovery after acceptor bleaching. The increase in emission at 480nm was $50 \pm 2\%$ after $>80\%$ bleaching of YFP (induced by 3-5 min continuous

illumination with $480 \pm 15 \text{ nm}$). To determine agonist-induced changes in FRET, cells were continuously superfused with buffer A and agonist was applied using a solenoid valve controlled rapid superfusion device (Bünemann *et al.*, 1997) (ALA-VM8, ALA Scientific Instruments). Signals detected by avalanche photodiodes were digitalized using a AD converter (Digidata1322A, Axon Instruments) and stored on PC using Clampex 8.1 software (Axon Instruments). The decrease in FRET ratio was fitted to the equation: $r(t) = A \times (1 - e^{-t/\tau})$, where τ is the time constant (s) and A is the magnitude of the signal. When necessary for calculating τ , agonist-independent changes in FRET due to photobleaching were subtracted.

Membrane preparation. Membrane fractions were obtained after two centrifugations at 4°C , first at $800 \times g$ for 10 min and the second at $100,000 \times g$ for 30 min. Membranes were treated with 6 M urea in 20 mM Hepes, pH 7.4, for 30 min on ice followed by centrifugation at $100,000 \times g$ for 15 min. After two washing steps at 4°C in buffer B the membranes were resuspended in a buffer A (without BSA) and immediately used in the experiments. 20 μl aliquots of membranes were subjected to fluorescence microscopy similar to intact cells using a 20x objective.

References

- Bockaert, J. and Pin, J. P. (1999) Molecular tinkering of G protein-coupled receptors: an evolutionary success. *EMBO J.*, **18**, 1723-1729.
- Bourne, H. R. (1997) How receptors talk to trimeric G proteins. *Curr. Opin. Cell Biol.*, **9**, 134-142.
- Bünemann, M., Brandts, B. and Pott, L. (1997) In vivo downregulation of M2 receptors revealed by measurement of muscarinic K⁺ current in cultured guinea-pig atrial myocytes. *J. Physiol.*, **501**, 549-554.
- Bünemann, M., Bücheler, M. M., Philipp, M., Lohse, M. J. and Hein, L. (2001) Activation and desactivation kinetics of α_{2A} - and α_{2C} -adrenergic receptor-activated G protein-activated inwardly rectifying K⁺ channel currents. *J. Biol. Chem.* **276**, 47512-47517.
- Farrens, D. L., Altenbach, C., Yang, K., Hubbell, W. L. and Khorana, H. G. (1996) Requirement of rigid-body motion of transmembrane helices for light activation of rhodopsin. *Science* **274**, 768-770.
- Gardella, T. J. and Jüppner, H. (2001) Molecular properties of the PTH/PTHrP receptor. *Trends Endocrinol. Metabolism.*, **12**, 210-217.
- Gether, U., Lin, S. B. and Kobilka, K. (1995) Fluorescent labeling of purified β_2 -adrenergic receptor: evidence for ligand-specific conformational changes. *J. Biol. Chem.*, **270**, 28268-28275.
- Gether, U. and Kobilka, B. K. (1998) G protein-coupled receptors. Mechanism of agonist activation. *J. Biol. Chem.*, **273**, 17979-17982.

- Gether, U. (2000) Uncovering molecular mechanism involved in activation of G protein-coupled receptor. *Endocr. Rev.*, **21**, 90-113.
- Ghanouni, P., Gryczynski, Z., Steenhuis, J. J., Lee, T. W., Farrens, D. L., Lakowicz, J. R., and Kobilka, B. K. (2001a) Functionally different agonists induce distinct conformations in the G protein coupling domain of the β_2 adrenergic receptor. *J. Biol. Chem.*, **276**, 24433-24436.
- Ghanouni, J., Steenhuis, J., Farrens, D. L. and Kobilka, B. K. (2001b) Agonist-induced conformational changes in the G-protein-coupling domain of the β_2 adrenergic receptor. *Proc. Natl. Acad. Sci. USA.*, **98**, 5997-6002.
- Greasley, P.J., Fanelli, F., Scheer, A., Abuin, L., Nenniger-Tosato, M., DeBenedetti, P.G., and Cotecchia, S. (2001) Mutational and computational analysis of the α_{1b} -adrenergic receptor. *J. Biol. Chem.*, **276**, 46485-46494.
- Groarke, D. A., Wilson, S., Krasel, C. and Milligan, G. (1999) Visualization of agonist-induced association and trafficking of green fluorescent protein-tagged forms of both β -arrestin-1 and the thyrotropin-releasing hormone receptor. *J. Biol. Chem.*, **274**, 23263-23269.
- Jensen, A. D., Guarnieri, F., Rasmussen, S. G. F., Asmar, F., Ballesteros, J. A., and Gether, U. (2001) Agonist-induced conformational changes at the cytoplasmic side of transmembrane segment 6 in the β_2 adrenergic receptor mapped by site-selective fluorescent labeling. *J. Biol. Chem.*, **276**, 9279-9290.
- Jüppner, H., Abou-Samra, A. B., Freeman, M., Kong, X. F., Schipani, E., Richards, J., Kolakowski, L. F., Jr., Hock, J., Potts, J. T., Jr., Kronenberg, H. M., and Segre, G. V. (1991) A G protein-linked receptor for parathyroid hormone and parathyroid hormone-related peptide. *Science*, **254**, 1024-1026.

- Lim, W. J. and Neubig, R. R. (2001) Selective inactivation of guanine-nucleotide-binding regulatory protein (G-protein) α and $\beta\gamma$ subunits by urea. *Biochem. J.*, **354**, 337-344.
- Miyawaki, A. and Tsien, R. Y. (2000) Monitoring protein conformations and interactions by fluorescence resonance energy transfer between mutants of green fluorescent protein. *Methods Enzymol.* **327**, 472-501.
- Okada, T., Ernst, O. P., Palczewski, K. and Hofmann, K. P. (2001) Activation of rhodopsin: new insights from structural and biochemical studies. *Trends Biochem. Sci.* **26**, 318-324
- Rohrer, D. K. and Kobilka, B. K. G protein-coupled receptors: functional and mechanistic insights through altered gene expression. *Physiol. Rev.* **78**, 35-52 (1998)
- Sheikh, S. P., Zvyaga, T. A., Lichtarge, O., Sakmar, T. P. and Bourne, H. R. (1996) Rhodopsin activation blocked by metal-ion-binding sites linking transmembrane helices C and F. *Nature* **383**, 347-350
- Sheikh, S. P., Vilardaga, J.P., Baranski, T. J., Lichtarge, O., Iiri, T., Meng, E. C., Nissenson, R. A., and Bourne, H. R. (1999) Similar structures and shared switch mechanisms of the β_2 -adrenoceptor and the parathyroid hormone receptor. *J. Biol. Chem.* **274**, 17033-17041
- Tsien, R. Y. (1998) The green fluorescent protein. *Annu. Rev. Biochem.*, **67**, 509-544.
- Vilardaga, J. P., di Paolo, E. and Bollen, A. (1995) Improved PCR method for high efficacy site-directed mutagenesis using class 2S restriction enzymes. *Biotechniques*, **18**, 605-606.

- Vilardaga, J. P., Frank, M., Krasel, C., Dees, C., Nissenson, R. A., and Lohse, M. J. (2001) Differential conformational requirements for activation of G proteins and regulatory proteins, arrestin and GRK in the parathyroid hormone receptor. *J. Biol. Chem.*, **276**, 33435-33443.
- Vilardaga, J. P., Krasel, C., Chauvin, S., Bambino, T., Lohse, M. J., and Nissenson, R. A. (2002) Internalization determinants of the parathyroid hormone receptor differentially regulates β -arrestin/receptor association. *J. Biol. Chem.*, **277**, 8121-8129.
- Ward, S. D. C., Hamdan, F. F., Bloodworth, L. M. and Wess, J. (2002) Conformational changes that occur during M_3 muscarinic acetylcholine receptor activation probed by the use of an in situ disulfide cross-linking strategy. *J. Biol. Chem.*, **277**, 2247-2257.
- Wieland, K., Zuurmond, H. M., Krasel, C., IJzerman, A. P. and Lohse, M. J. (1996) Involvement of Asn-293 in stereospecific agonist recognition and in activation of the β_2 -adrenergic receptor. *Proc. Natl. Acad. Sci. USA* **93**, 9276-9281.

Acknowledgements

We thank Manfred Bernhard for support with the radioligand binding studies and Christian Dees for the G protein preparation. We are grateful to Dr. Martin Heck for help with computer simulations and Drs. Ernst J.M. Helmreich, Lutz Hein, Ursula Quitterer and Henry R. Bourne for critical comments on the manuscript. This work was supported by the Deutsche Forschungsgemeinschaft and the Fonds der Chemischen Industrie (grants to M.J.L.).

Legends to figures

Figure 1. FRET efficiency and time-resolved changes in the FRET signal of PTHR-cam. (A) Overall transmembrane topology of the GPCR-cam constructs. (B) Fluorescence emission spectra of selected PTHR constructs. Shown are the emission spectra of PTHR-CFP_{3-loop} (blue), PTHR-YFP_{C-term} (yellow) and PTHR-cam (red) upon excitation at 433 nm. (C) Effects of photobleaching. Emission intensities of YFP (535 nm, yellow), CFP (480 nm, blue) and the ratio F^*_{535}/F^*_{480} (red) were recorded simultaneously from single cells expressing PTHR-cam using fluorescence microscopy. Emission intensities and the ratio F^*_{535}/F^*_{480} were recorded before and after the acceptor fluorophore was photobleached by 5 min exposure to light at 480 nm. (D) Time-resolved changes in the ratio F^*_{535}/F^*_{480} in single HEK293 cells stably expressing PTHR-cam. Emission intensities of YFP (535 nm, yellow), CFP (480 nm, blue) and the ratio F^*_{535}/F^*_{480} (red) were recorded simultaneously from single cells. Shown are the changes induced by rapid superfusion with 1 μ M PTH (arrow). The decrease of the ratio F^*_{535}/F^*_{480} was fitted by a simple mono-exponential curve giving a time-constant in this experiment of 3.5 s. Changes in the ratio are expressed as % decrease from the initial value at $t=0$ s.

Figure 2. Pharmacological properties of the GPCR-cam constructs.

(A-B) Comparison between the binding and signalling properties of PTHR-cam (A), α_{2A} -AR-cam (B) and their respective wild type receptor stably expressed in HEK293 cells. The data are the means \pm S.E. of at least 4 separate experiments carried out in

duplicate. (C) Visualization PTHR-cam stably expressed in HEK293 cells by confocal microscopy.

Figure 3. Agonist-induced decrease in FRET signal corresponds to receptor activation. (A) *Intact cell* panel shows the effects of the agonist PTH (1 μ M) and the antagonist PTH(7-34) (3 μ M) on the ratio F_{535}^*/F_{480}^* of PTHR-cam in intact HEK293 cells. *Membranes* panel shows the effects of PTH (1 μ M) in cell membranes prepared from HEK293 cells stably expressing PTHR-cam. The membranes were measured either without further treatment (left), or after treatment with 6 M urea (right). Bars represent the % decrease in the ratio F_{535}^*/F_{480}^* upon PTH exposure. (B) Effect of the antagonist phentolamine (10 μ M) on the FRET signal caused by 10 μ M noradrenaline (NA) in HEK293 cells stably expressing α_{2A} AR-cam (n=4). (C) Comparison of the guanine nucleotide sensitivity of the FRET signal (*left* panel) and agonist binding (*right* panel) evoked by sub-saturating concentration of UK14304 in membranes containing α_{2A} AR-cam in the presence of G_o proteins (ratio receptor: G_o 1:100) with or without GTP γ S (10 μ M). Data are the means \pm S.E. of at least 4 separate experiments.

Figure 4. Action of the partial agonist clonidine on α_{2A} AR-cam. Changes in FRET in response to 10 μ M noradrenaline (NA) or 10 μ M clonidine added alone or together were recorded in a single HEK293 cell expressing α_{2A} AR-cam. The recording is representative of 4 independent experiments.

Figure 5. Comparison between the dynamics of receptor activation and desensitization of PTHR-cam. The kinetics of activation of PTHR-cam and of β -arrestin2-YFP binding to the PTHR-CFP_{C-term} were measured as changes in the ratio F^*_{535}/F^*_{480} in cells expressing PTHR-cam or co-expressing PTHR-CFP_{C-term} and β -arrestin2-YFP in response to 100 nM PTH. The recordings are expressed as % of the respective maximal response and are representative of at least 3 independent experiments. Note that in the case of PTHR-CFP_{C-term}/ β -arrestin2-YFP the ratio F^*_{535}/F^*_{480} does indeed increase, while in the PTHR-cam the ratio decreases and is depicted as a positive signal just to facilitate the comparison of the kinetics. The *inset* represents a time scale expansion to illustrate the differences in response delays.

Figure 6. Dynamics of agonist-mediated receptor conformational change. (A) Time-resolved changes in the ratio F^*_{535}/F^*_{480} of the PTHR-cam (*left* panel) and α_{2A} AR-cam (*right* panel) expressed in HEK293 cells at various concentrations of PTH and norepinephrine, respectively. (B) Relationship between the apparent rate constant, k_{obs} and agonist concentration. k_{obs} -values were also obtained from fitting the kinetic data of Figure 6A with a mono-exponential equation. At low concentrations of agonist, k_{obs} -values were directly proportional to the agonist-concentration, whereas at higher concentrations of agonist the values approached a maximal value of about 1 s^{-1} and 26 s^{-1} for PTHR-cam and α_{2A} AR-cam, respectively. Note that the k_{obs} values depicted in Fig. 6B saturated at much higher ligand concentrations than the binding data shown in Fig. 2. This is due to the fact that the k_{obs} values are not measured at equilibrium. Data indicate the mean \pm SEM of at least 7 separate experiments.

Supplementary data

Suppl. Figure 1. Guanine nucleotide sensitivity of agonist binding at the α_{2A} AR-cam stably expressed in HEK-293 cells. In the presence of exogenous G_o protein (at a molar ratio 1:100, receptor: G_o) the binding affinity for the α_{2A} AR agonist UK14,304 for membranes containing α_{2A} AR-cam decreases ≈ 3 -fold in presence of 10 μ M GTP γ S ($K_d=3.4\pm 0.8$ nM vs $K_d=9.6\pm 1.1$ nM, $n=3$) reflecting the shift of the receptor population to a lower affinity state.

Figure 1 (Villardaga et al.)

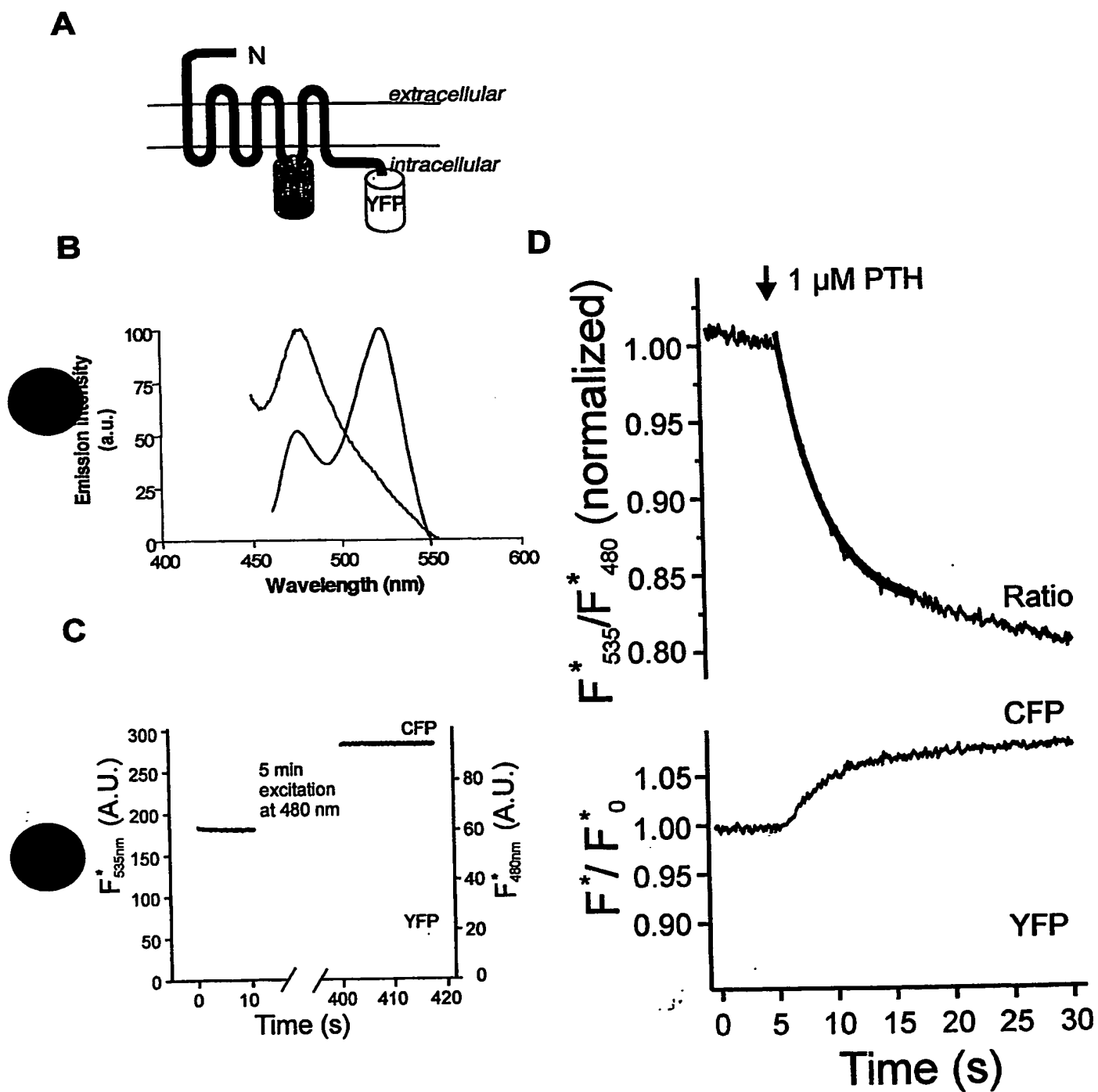


Figure 2 (Vilardaga et al.)

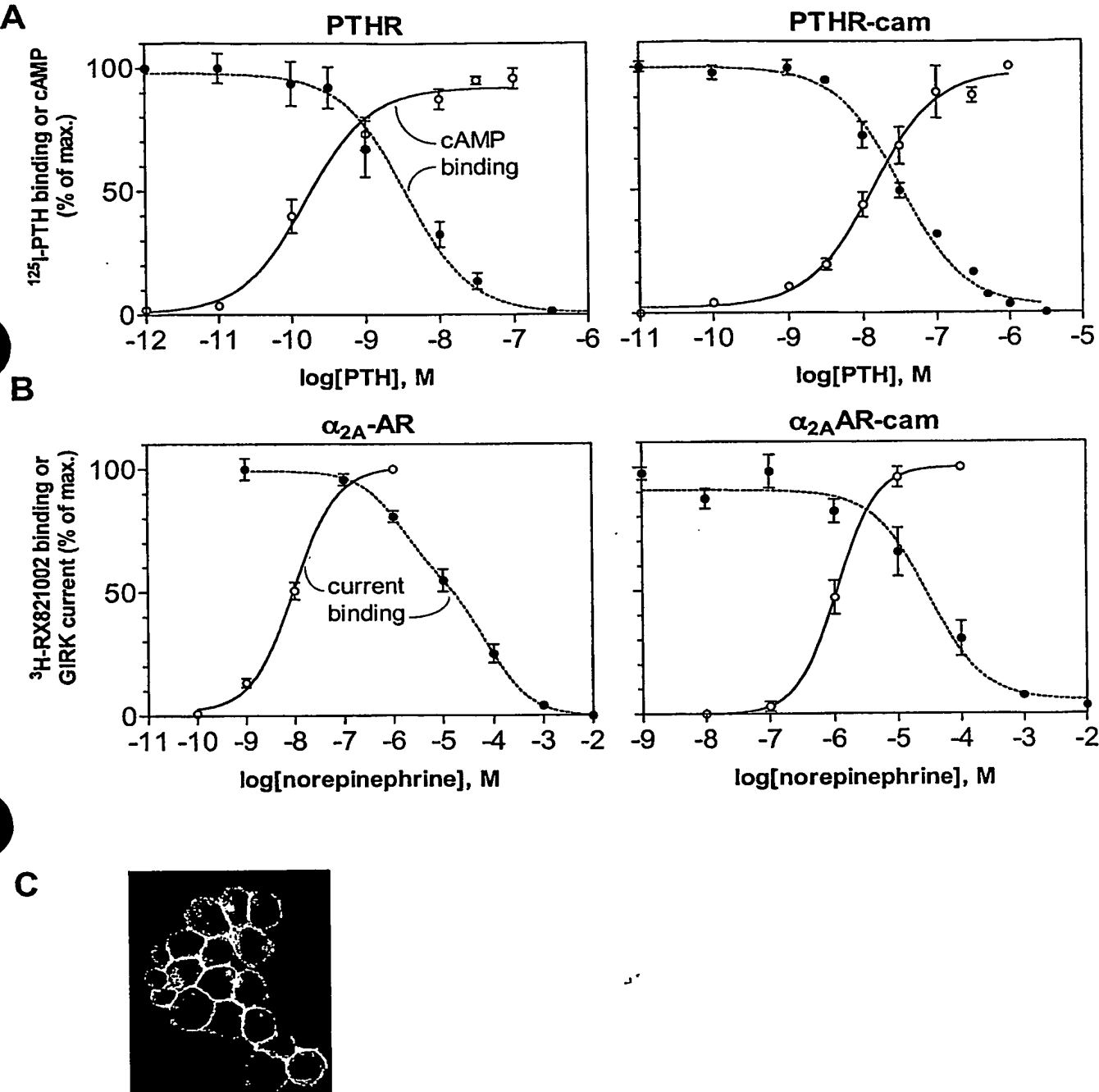


Figure 3 (Vilardaga et al.)

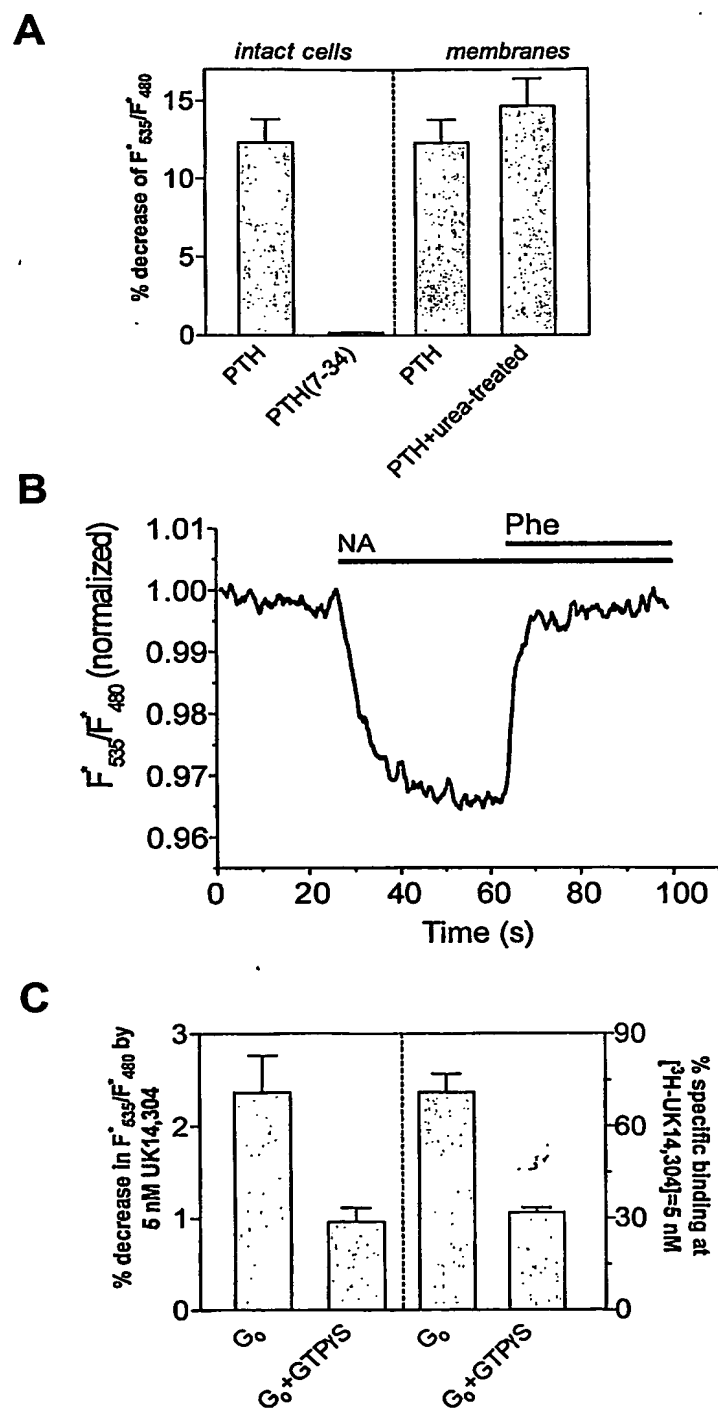


Figure 4 (Vilardaga et al.)

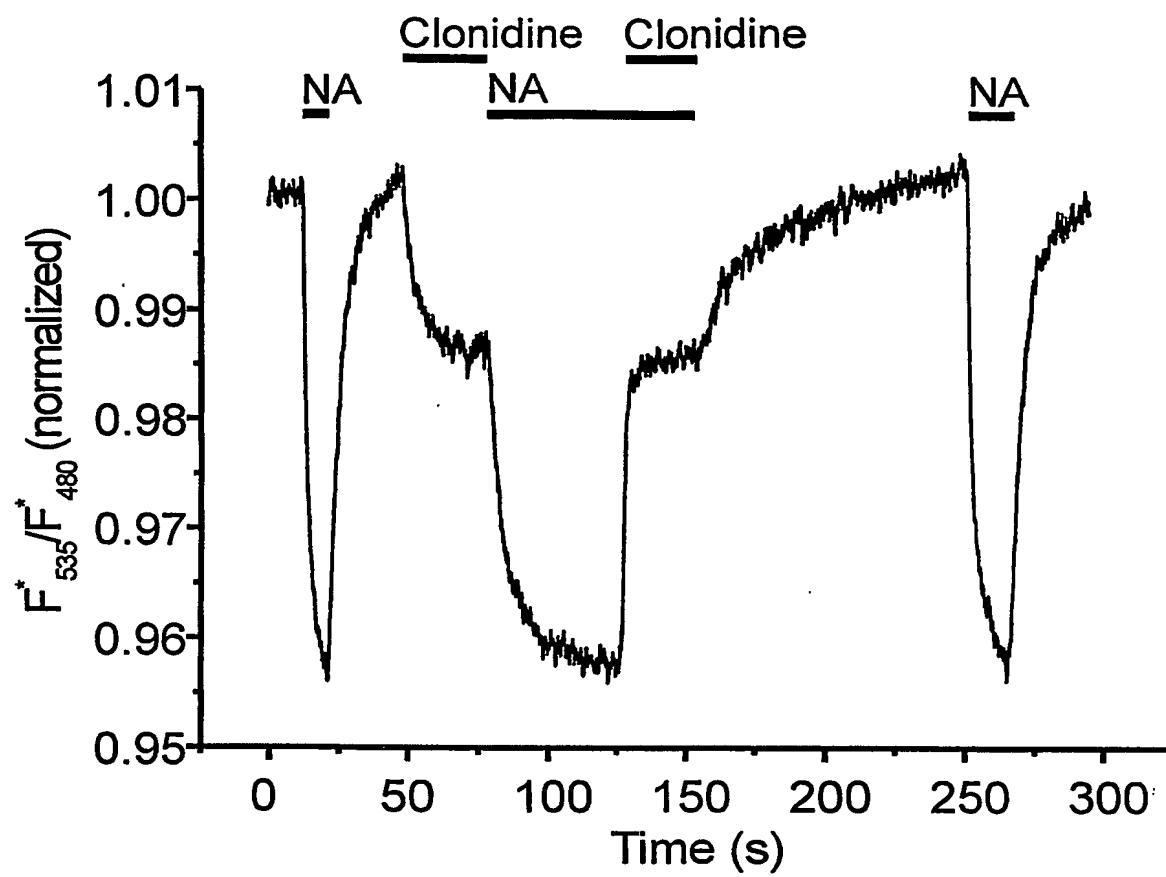


Figure 5 (Vilardaga et al.)

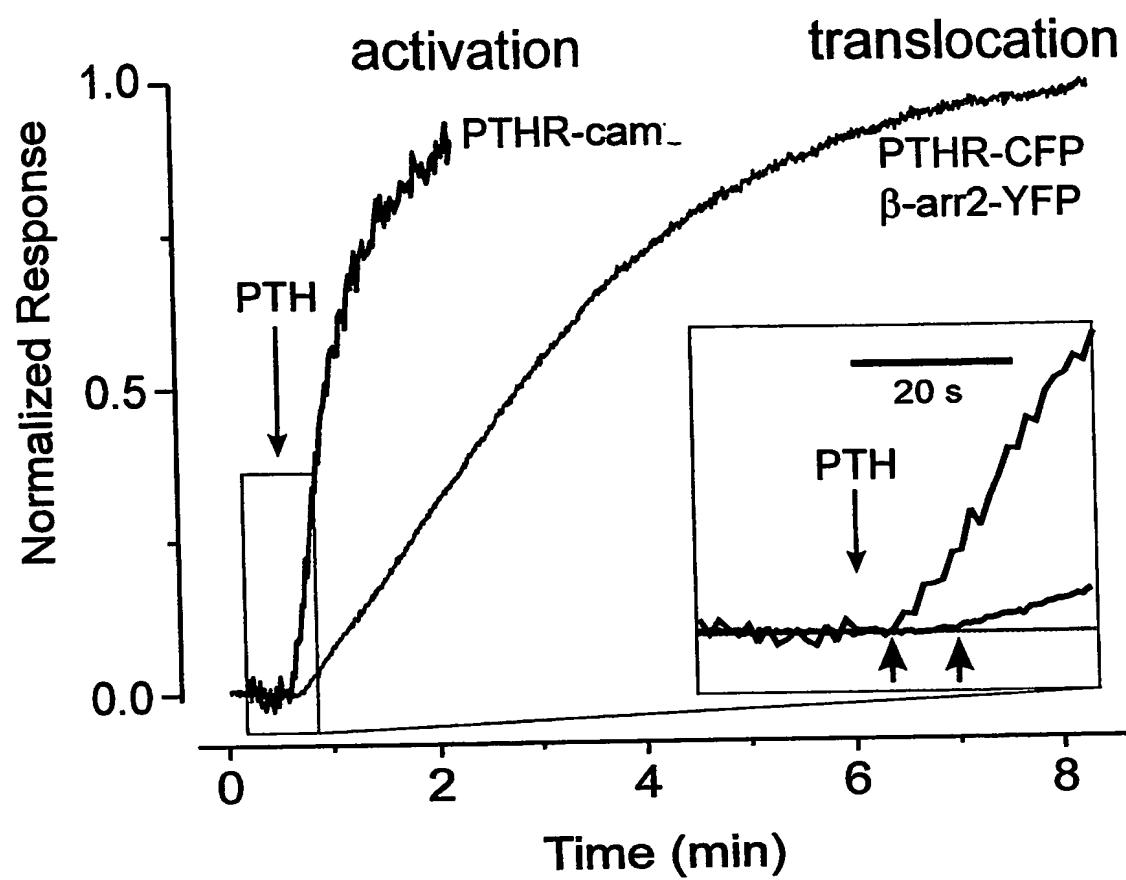
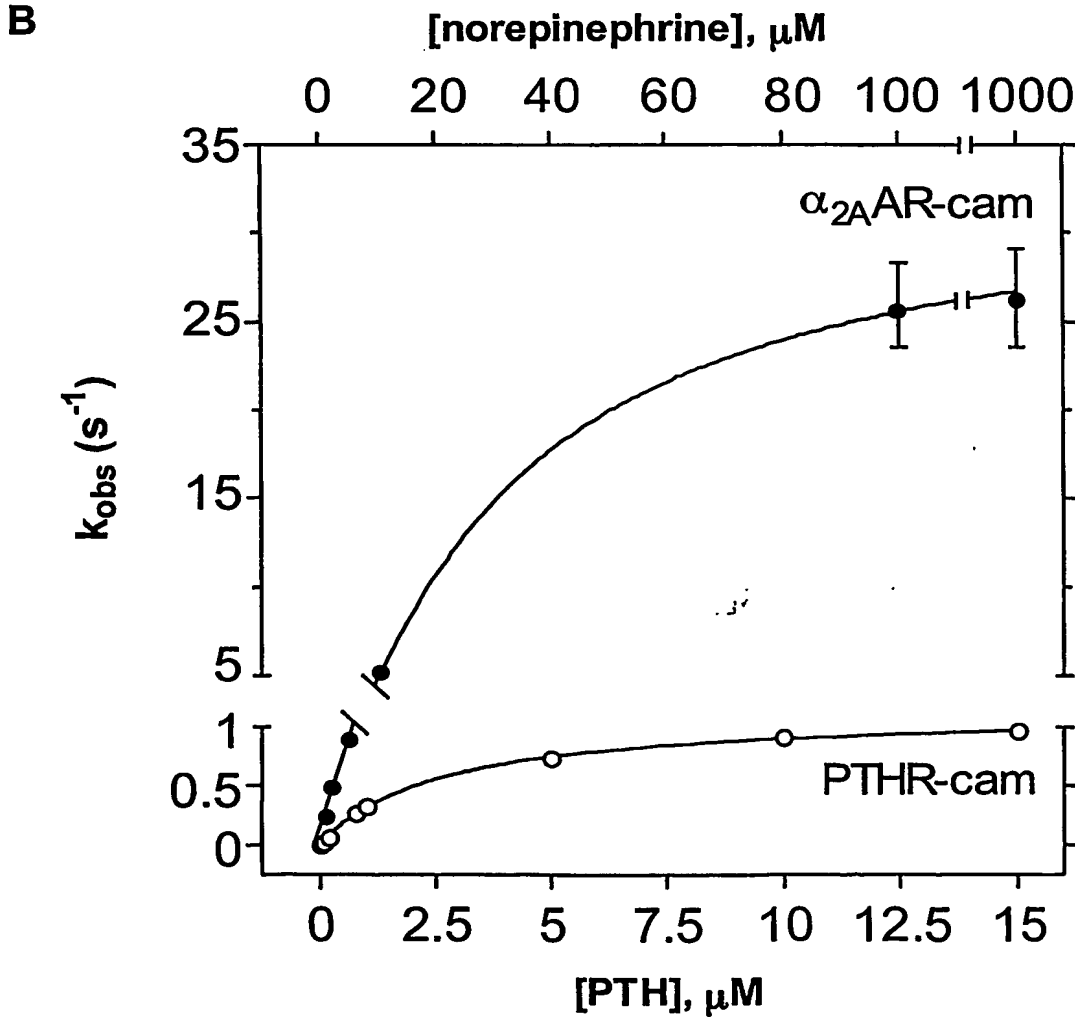
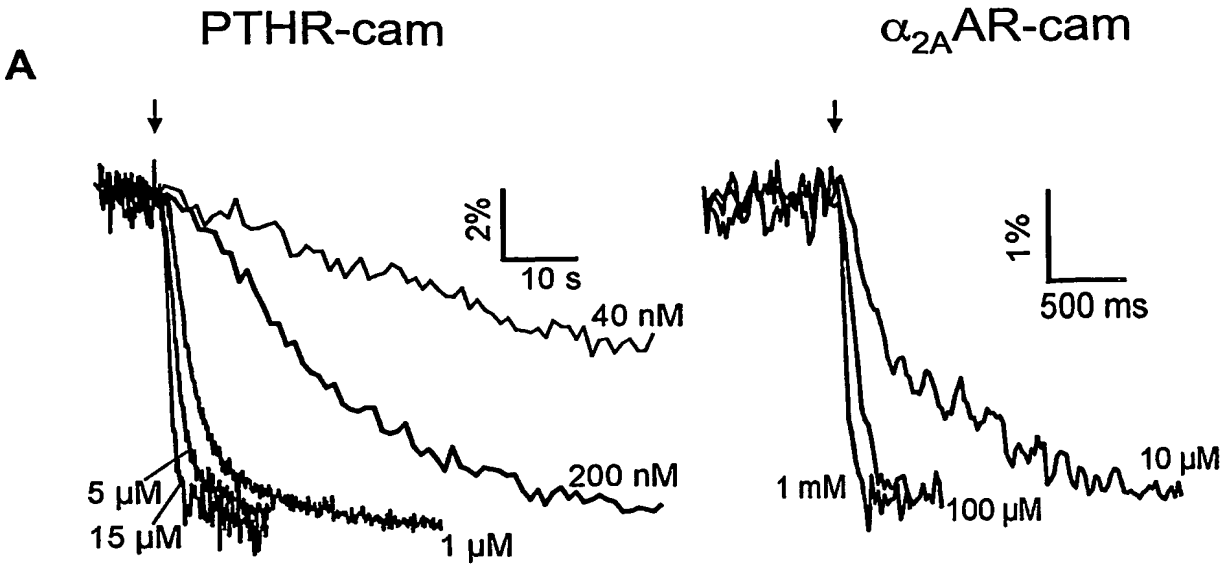
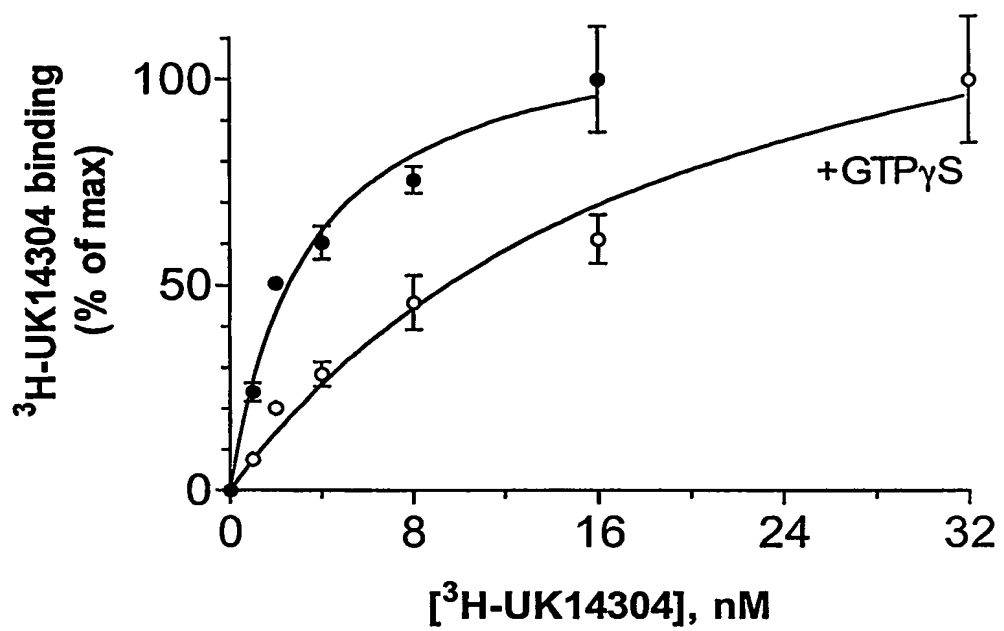


Figure 6 (Villardaga et al.)



Suppl. Figure 1 (Vilardaga et al.)



**This Page is Inserted by IFW Indexing and Scanning
Operations and is not part of the Official Record**

BEST AVAILABLE IMAGES

Defective images within this document are accurate representations of the original documents submitted by the applicant.

Defects in the images include but are not limited to the items checked:

- ☐ BLACK BORDERS
- ☐ IMAGE CUT OFF AT TOP, BOTTOM OR SIDES
- ☐ FADED TEXT OR DRAWING
- ☒ BLURRED OR ILLEGIBLE TEXT OR DRAWING
- ☒ SKEWED/SLANTED IMAGES
- ☐ COLOR OR BLACK AND WHITE PHOTOGRAPHS
- ☐ GRAY SCALE DOCUMENTS
- ☐ LINES OR MARKS ON ORIGINAL DOCUMENT
- ☒ REFERENCE(S) OR EXHIBIT(S) SUBMITTED ARE POOR QUALITY
- ☐ OTHER: _____

IMAGES ARE BEST AVAILABLE COPY.

As rescanning these documents will not correct the image problems checked, please do not report these problems to the IFW Image Problem Mailbox.